

## Latest Results from CERES/NA45

Johannes P. Wessels<sup>a</sup> for the CERES/NA45 Collaboration

D. Adamová<sup>b</sup>, G. Agakichiev<sup>a</sup>, H. Appelshäuser<sup>c</sup>, V. Belaga<sup>d</sup>, P. Braun-Munzinger<sup>a</sup>, R. Campagnolo<sup>c</sup>, A. Castillo<sup>a</sup>, A. Cherlin<sup>e</sup>, S. Damjanović<sup>c</sup>, T. Dietel<sup>c</sup>, L. Dietrich<sup>c</sup>, A. Drees<sup>f</sup>, S. I. Esumi<sup>c</sup>, K. Filimonov<sup>c</sup>, K. Fomenko<sup>d</sup>, Z. Fraenkel<sup>e</sup>, C. Garabatos<sup>a</sup>, P. Glässel<sup>c</sup>, G. Hering<sup>a</sup>, J. Holeczek<sup>a</sup>, V. Kushpil<sup>b</sup>, B. Lenkeit<sup>g</sup>, W. Ludolphs<sup>c</sup>, A. Maas<sup>a</sup>, A. Marín<sup>a</sup>, F. Messer<sup>f</sup>, J. Milošević<sup>c</sup>, A. Milov<sup>e</sup>, D. Miśkowiec<sup>a</sup>, L. Musa<sup>g</sup>, Yu. Panebrattsev<sup>d</sup>, O. Petchenova<sup>d</sup>, V. Petráček<sup>c</sup>, A. Pfeiffer<sup>g</sup>, J. Rak<sup>h</sup>, I. Ravinovich<sup>e</sup>, P. Rehak<sup>i</sup>, M. Richter<sup>c</sup>, H. Sako<sup>a</sup>, W. Schmitz<sup>c</sup>, J. Schukraft<sup>g</sup>, S. Sedykh<sup>a</sup>, W. Seipp<sup>c</sup>, A. Sharma<sup>a</sup>, S. Shimansky<sup>d</sup>, J. Slívová<sup>c</sup>, H. J. Specht<sup>c</sup>, J. Stachel<sup>c</sup>, M. Šumbera<sup>b</sup>, H. Tilsner<sup>c</sup>, I. Tserruya<sup>e</sup>, J. P. Wessels<sup>a</sup>, T. Wienold<sup>c</sup>, B. Windelband<sup>c</sup>, J. P. Wurm<sup>h</sup>, W. Xie<sup>e</sup>, S. Yurevich<sup>c</sup>, V. Yurevich<sup>d</sup>

<sup>a</sup>GSI, Darmstadt, Germany

<sup>b</sup>NPI ASCR, Řež, Czech Republic

<sup>c</sup>Heidelberg University, Germany

<sup>d</sup>JINR Dubna, Russia

<sup>e</sup>Weizmann Institute, Rehovot, Israel

<sup>f</sup>SUNY at Stony Brook, U.S.A.

<sup>g</sup>CERN, Geneva, Switzerland

<sup>h</sup>MPI, Heidelberg, Germany

<sup>i</sup>BNL, Upton, U.S.A.

In this talk latest results from the analysis of  $e^+e^-$ -pairs emitted in Pb+Au collisions at 40 AGeV/c and a combined analysis of all data available at 158 AGeV/c are presented. The enhancement of low-mass  $e^+e^-$ -pairs ( $m_{ee} > 0.2 \text{ GeV}/c^2$ ) with respect to the expected yield from hadron decays first reported at 158 AGeV/c is also found at 40 AGeV/c and is even larger there. Comparing to various theoretical models based on  $\pi^+\pi^-$  annihilation, the data can only be reproduced, if the properties of the intermediate  $\rho$  in the hot and dense medium are modified. Theoretically, the modification is linked to baryon density rather than temperature. Constraints from hadron data taken at the same beam energies indeed indicate a fireball evolution along a trajectory of higher baryon density at 40 AGeV/c, consistent with the observed larger enhancement factor.

## 1. INTRODUCTION

Along with the deconfinement phase transition to the quark gluon plasma (QGP), chiral symmetry is expected to be restored. The energy density at which the phase transition is predicted by two-flavor lattice calculations is  $\epsilon \approx 0.7 \text{ GeV/fm}^3$  [ 1] with large errors due to uncertainties in the critical temperature. Simple estimates employing the Bjorken expansion scenario [ 2] show that the initial energy density reached in central Pb+Pb collisions is about  $3 \text{ GeV/fm}^3$  at the full SPS energy. The totality of the observables has led to the announcement that a new state of matter is indeed formed in central heavy ion collisions at the SPS [ 3]. The measurement of  $e^+e^-$ -pairs is particularly well suited to study this matter since they are emitted throughout the entire collision and are themselves not subject to the strong final state interaction. In this context, the decay of the  $\rho$  vector meson into  $e^+e^-$ -pairs is of particular interest, due to its direct link to chiral symmetry restoration. Because of the short lifetime (1.3 fm/c),  $e^+e^-$ -pairs from  $\rho$  decays are dominated by decays within the hot and dense medium, directly mirroring its properties. Experimentally, however, the study of  $e^+e^-$ -pairs is notoriously difficult, because of the small production cross section as well as the large combinatorial background in heavy ion collisions.

In the following we briefly describe the experimental setup, followed by a description of the electron analysis procedure. We then present results from a combined analysis of all the data that were taken at the full SPS energy of 158 AGeV. Then the final results of the data taken at 40 AGeV are shown. We conclude after a comparison of the data to models and a discussion of the fireball evolution.

## 2. CERES SETUP

The CERES spectrometer is optimized to measure  $e^+e^-$ -pairs in the mass range up to about  $1 \text{ GeV}/c^2$  in the range  $2.1 < \eta < 2.65$  close to midrapidity. A cross section through the azimuthally symmetric setup is shown in Figure 1.

A segmented micro target (8 disks of Au of  $25 \mu\text{m}$  thickness and  $600 \mu\text{m}$  diameter evenly spaced along 22 mm) is followed by a set of two **Silicon Drift Detectors** (SDD1/SDD2) at a distance of 10 cm and 13 cm respectively. The segmentation minimizes conversions of photons in the target. The set of silicon drift detectors provides precise determination of the angles of all charged particles, determination of the event vertex, and the total charged particle multiplicity for each event. Along with the position measurement the specific energy loss is recorded for each charged particle.

Electrons are identified with two **Ring Imaging Cherenkov** counters (RICH1/2) which are operated at a threshold of  $\gamma_{th} = 32$  suppressing more than 99% of all charged hadrons. In 1995/96 the spectrometer was operated with a radial magnetic field provided by two air coils with counter-running current in between the two RICHes [ 4]. With this setup a mass resolution of about 5.7% was reached in the mass region of the  $\rho/\omega$ .

For the runs in 1999/2000 the experiment was upgraded by the addition of a radial TPC [ 5] inside a separate radial magnetic field ( $B_{\text{max}}=0.5 \text{ T}$ ). Over the total length of 2 m a maximum of 20 hits are recorded for each charged particle track. In the 1999 analysis a mass resolution of about 4.2% was achieved in the  $\rho/\omega$  region. For the 2000 data the goal is to reach with better calibration about 2%. For runs with the TPC the

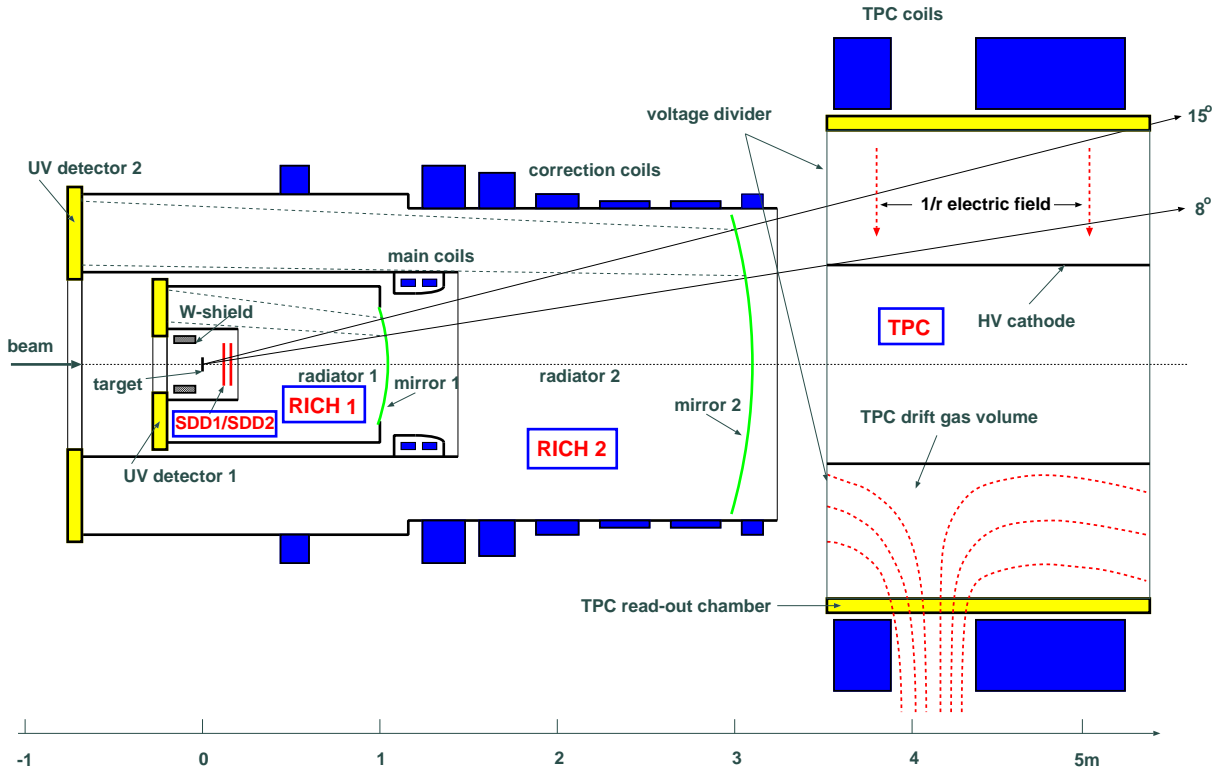


Figure 1. Cross section through the upgraded setup of the CERES spectrometer

magnetic field between the RICHes was switched off and electrons were identified by combining the two RICHes, improving the electron efficiency to about 90% (as compared to about 70% in 1995/1996).

A compilation of all Pb+Au events taken with different configurations of the CERES spectrometer is shown in Table 1.

The data taken in 1995 and 1996 used the original CERES setup without the TPC. All data taken thereafter employed the upgraded setup shown in Figure 1. The new read-out of the experiment was only partially operational for the low energy run at 40 AGeV/c in 1999 limiting both statistics and performance. The large data sample taken in 2000 at the full SPS energy is still being analyzed.

### 3. ELECTRON ANALYSIS

While  $e^+e^-$ -pairs are an attractive probe, they are notoriously hard to measure due to the small production cross section and the enormous combinatorial background from unrecognized photon conversions and  $\pi^0$  Dalitz decays. The analysis steps for the 1995/96 data are detailed in Ref. [12]. Here, we only describe the analysis of data taken with the TPC and the field between the RICHes turned off. Electron candidates are selected when ten or more photon hits in RICH1 and RICH2 form a ring with asymptotic radius. To those candidates a transverse momentum cut of 200 MeV/c is applied reducing contributions from  $\pi^0$  Dalitz decays and conversions by about a factor of 10. Electron identification is further improved, removing high- $p_t$  pions and accidental matches between

Table 1

Number of collected Pb+Au events along with the respective trigger cross sections.

Year	$p_{beam}$	$\sigma/\sigma_{geo}$	Events
1995	158 AGeV/c	35%	$8.5 \cdot 10^6$
1996	158 AGeV/c	30%	$43 \cdot 10^6$
1999	40 AGeV/c	30%	$8 \cdot 10^6$ - partial readout
2000	80 AGeV/c	<30%	$0.5 \cdot 10^6$
	158 AGeV/c	8(25)%	$33(3.4) \cdot 10^6$

the RICHes and the TPC, by a cut on specific energy loss in the TPC vs. momentum as shown in Figure 2. Those conversions and Dalitz pairs with very small opening angles that do not lead to separate rings in the RICHes are efficiently removed by rejecting tracks with large specific energy loss in both silicon drift detectors as shown in Figure 3. Further, electron candidates without a match in the TPC within 70 mrad of an electron track are also removed. The complete set of cuts employed in the analysis is shown in detail in Ref. [ 6, 7, 8]. Finally, the invariant mass spectrum of  $e^+e^-$ -pairs is obtained by subtracting twice the geometric average of the remaining like-sign pairs from the remaining unlike-sign pairs ( $N_{e^+e^-} - 2\sqrt{N_{e^+e^+} \cdot N_{e^-e^-}}$ ).

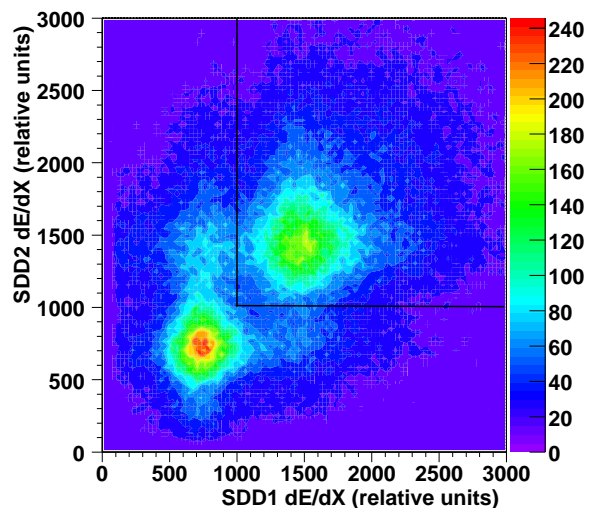


Figure 2. Specific energy loss in the TPC for electron candidates identified with the RICHes. The indicated cut was used to efficiently reject a remaining contamination from pion tracks. The cut at  $p=1$  GeV/c corresponds to the  $p_t$ -cut of 0.2 GeV/c.

Figure 3. Specific energy loss for charged particle tracks in the two silicon drift detectors. The cut indicates unresolved pairs of tracks mostly due to conversions.

## 4. Pb+Au AT 158 AGeV/c

### 4.1. Invariant mass spectrum of $e^+e^-$ -pairs

Analyses of the invariant mass spectra of  $e^+e^-$ -pairs from the runs in 1995/1996 have been published [ 9, 10, 11]. In all cases cuts on the pair opening angle ( $\Theta_{ee} > 35$  mrad) and the transverse momentum of the single electron track ( $p_t > 200$  MeV/c<sup>2</sup>) have been applied, and the spectra were compatible within their respective statistical and systematic errors. Recently [ 12] the data of 1995 and 1996 were combined in a unified analysis approach. For the two runs the trigger cross-section was slightly different. The cross section for the combined data corresponds to the 32% most central events. The average charged particle multiplicity is  $\langle N_{ch} \rangle = \langle dN_{ch}/d\eta \rangle \cdot \Delta\eta = 245 \cdot 0.55 = 135$  for the quoted rapidity interval. Since the efficiency for detecting  $e^+e^-$ -pairs depends on multiplicity, an efficiency correction is applied on an event-by-event basis. In the combination, the data were averaged bin-by-bin with weights according to the inverse squares of the relative errors of the individual measurements.

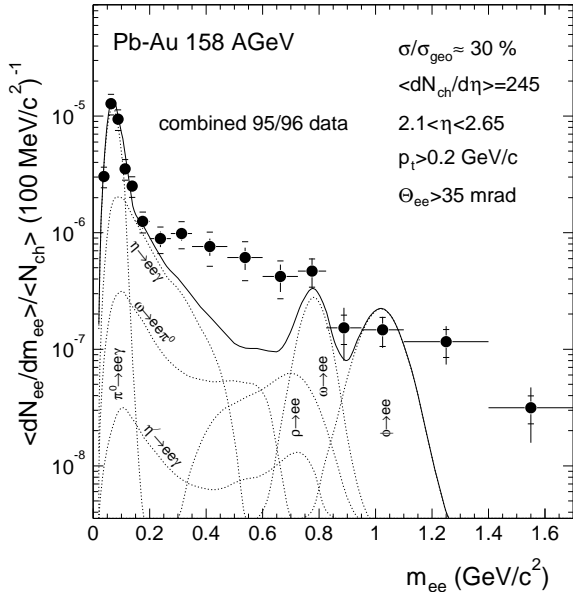


Figure 4. Invariant mass spectrum of  $e^+e^-$ -pair emitted in 158 AGeV/c Pb+Au collisions from the combined analysis of 1995 and 1996 data. The solid line shows the expected yield from hadron decays, dashed lines indicate the individual contributions to the total yield. See text for a discussion of systematic errors.

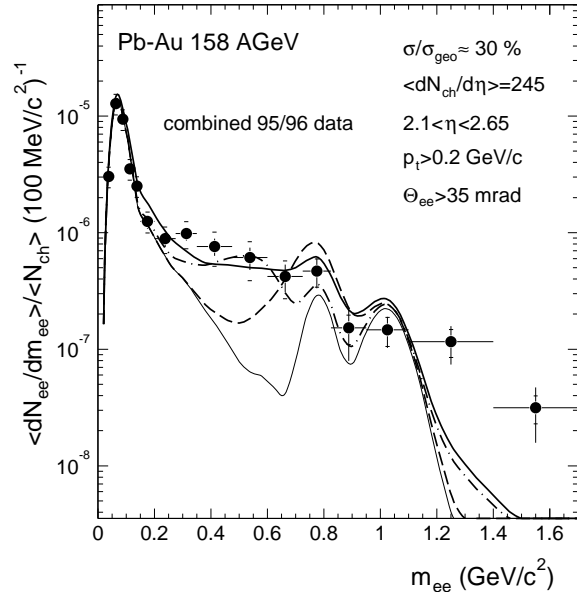


Figure 5. Comparison of the experimental data to i) free hadron decays without  $\rho$  decays (thin solid line), ii) model calculations with a vacuum  $\rho$  spectral function (thick dashed line), iii) with dropping in-medium  $\rho$ -mass (thick dash-dotted line, iv) with a medium-modified  $\rho$  spectral function (thick solid line).

The combined data are shown in Figure 4. The yield of pairs with  $m_{ee} > 0.2$  GeV/c<sup>2</sup> for the entire data sample is  $2666 \pm 260$  with a signal-to-background ratio of 1/12. On top of

the statistical errors, the spectrum has systematic errors of 20% for  $m_{ee} < 0.2$  GeV/ $c^2$  and 28% on average for  $m_{ee} > 0.2$  GeV/ $c^2$ , larger here due to the background subtraction and smoothing procedure. The background smoothing procedure introduces an additional 7% uncertainty in the overall normalization of the spectrum for  $m_{ee} > 0.2$  GeV/ $c$ . A detailed description of all errors can be found in Ref. [ 8, 12]

In Figure 4 the data are compared to the yield from hadron decays obtained from a *cocktail* containing particle ratios from a statistical model fitted to measured particle ratios in Pb+Pb collisions. Rapidity and transverse momentum distributions of the particles are taken from systematics of Pb+Pb collisions. The resulting distribution has been folded with the experimental mass resolution (5.7% in the  $\omega$  region). In the region  $m_{ee} > 0.2$  GeV/ $c^2$  the data exceed the yield from the *cocktail* by a factor of  $2.3 \pm 0.2(\text{stat}) \pm 0.6(\text{syst})$ . An additional systematic error of 0.7 is connected to the decay *cocktail*. The enhancement is not observed in proton induced reactions [ 13].

An independent analysis was performed using event mixing to generate the background [ 14]. The shape of this background is found to be identical to that of like-sign pairs, and the resulting invariant mass spectrum agrees well with the one in Figure 4. In addition, a lower single electron  $p_t$ -cut  $> 100$  MeV/ $c^2$  was used resulting in a factor of two more statistics for  $e^+e^-$ -pair masses above 0.2 GeV/ $c^2$  at a factor of three worse signal-to-background ratio. Again the resulting invariant mass spectrum agrees well with the one shown in Figure 4.

In Figure 5 the data are compared to the yield from various models based on  $\pi^+\pi^-$  annihilation with an intermediate  $\rho$  vector meson. The hadron decay *cocktail* is added without any contribution from the  $\rho$  to avoid double counting (thin line). Using the vacuum  $\rho$  spectral function produces the thick dashed line. The other two model calculations both contain modifications of the  $\rho$  spectral function. They involve in-medium  $\rho$  spectral functions with either a dropping  $\rho$  mass [ 15] (thick dash-dotted line) or with a spread  $\rho$  width [ 16] (thick line). Clearly, a modification of the  $\rho$  properties in the medium is needed to reach agreement with the experimental data. Unfortunately, the data do not allow to discern between the two different scenarios.

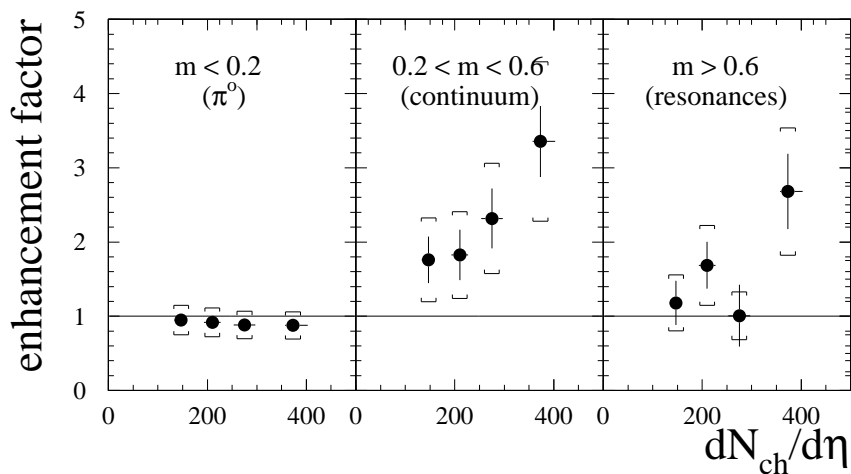


Figure 6. Enhancement of  $e^+e^-$  pairs from Pb+ Au collisions at 158 AGeV/ $c$  with respect to the yield expected from the hadron decay *cocktail* as a function of multiplicity and pair mass.

## 4.2. Multiplicity dependence of the enhancement

The combined data sample was subdivided into four different multiplicity bins. For each of these bins and for three different intervals in invariant mass, the ratio of the integral yield of  $e^+e^-$ -pairs to the expected yield from the hadron decay *cocktail* was evaluated. The results are shown in Figure 6. The mass region below  $0.2 \text{ GeV}/c^2$ , dominated by  $\pi^0$  Dalitz decays, is well reproduced by the *cocktail* for all centralities. In the mass region  $0.2 \text{ GeV}/c^2 < m_{ee} < 0.6 \text{ GeV}/c^2$  the enhancement with respect to the *cocktail* rises approximately linearly with multiplicity indicating that the rise of the integrated  $e^+e^-$ -pair yield is consistent with a quadratic multiplicity dependence; this is roughly expected for a two-body process like  $\pi^+\pi^-$  annihilation.

## 5. Pb+Au AT 40 AGeV/c

In 1999 the SPS delivered a 40 AGeV/c Pb-beam when the upgraded CERES spectrometer had just been commissioned. Preliminary results of what is presented in the following have already previously been shown [ 6, 7]. The data contain central events with an average multiplicity density at this energy of  $\langle dN_{ch}/d\eta \rangle = 216$ .

### 5.1. Invariant mass spectrum of $e^+e^-$ -pairs

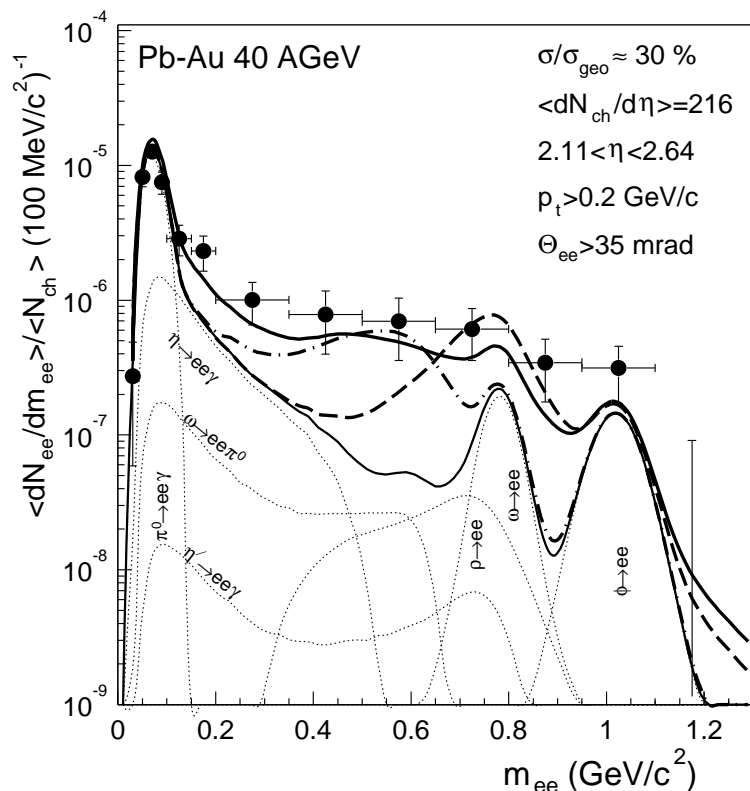


Figure 7.  $e^+e^-$ -pair mass spectrum from Pb+Au collisions at 40 AGeV/c compared to free hadron decays and various model calculations (line codes as in Fig. 5). Errors shown are only statistical, see text for a discussion of systematic errors.

The analysis leading to the invariant mass spectrum for the 40 AGeV/c data shown in Figure 7 has been outlined in Section 3 and is described in detail in [ 8]. The resulting

spectrum contains  $249 \pm 28$   $e^+e^-$ -pairs in the mass range below  $0.2 \text{ GeV}/c^2$  at a signal-to-background ratio of 1/1. The integrated yield for high mass pairs above  $0.2 \text{ GeV}/c^2$  is  $185 \pm 48$  pairs at a signal-to-background ratio of 1/6. The systematic errors are 16% and 20% for the low and high mass region, respectively.

For the comparison to the hadron decay *cocktail* the particle ratios have again been taken from statistical model fits adjusted to measured ratios from Pb+Pb collisions at 40 AGeV/c. Also the rapidity distributions and transverse momentum spectra follow the systematics of measurements at 40 AGeV/c. Again the cocktail has been folded with the experimental mass resolution (4.2% in the  $\omega$  region).

In the low mass region  $m_{ee} < 0.2 \text{ GeV}/c^2$  excellent agreement between the data and the *cocktail* is obtained. Here the ratio of data/decays is  $0.98 \pm 0.11(\text{stat}) \pm 0.16(\text{syst})$ . In the high mass region  $m_{ee} > 0.2 \text{ GeV}/c^2$ , however, the data exceeds the *cocktail* by a factor of  $5.1 \pm 1.3(\text{stat}) \pm 1.0(\text{syst})$  with an additional systematic error of 1.5 from the *cocktail*. This enhancement is larger than that observed at full SPS energy as quoted above, while the yield itself is not much larger than at 158 AGeV/c. Note that in the comparison of the enhancement factors between the two energies the additional systematic uncertainty from the *cocktail* essentially drops out.

Along with the data, model *predictions* [ 18] are presented for this energy. Again, a treatment of the  $\rho$  unmodified by medium effects is clearly ruled out. However, once more the data do not allow to discern the two scenarios involving in-medium modifications of the  $\rho$  propagator with a shifted mass, i.e. *Brown/Rho scaling* [ 15, 18], or with a spread width [ 18].

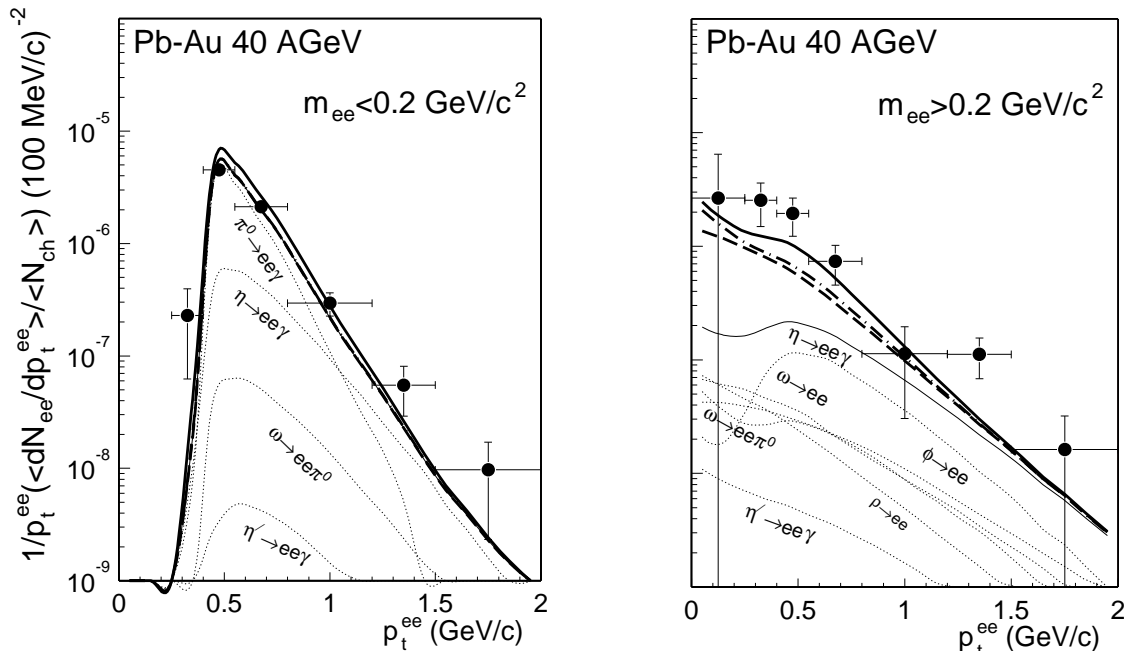


Figure 8. Invariant pair- $p_t^{ee}$  spectra for  $e^+e^-$ -pair masses  $m_{ee} < 0.2 \text{ GeV}/c^2$  (left panel) and  $m_{ee} > 0.2 \text{ GeV}/c^2$  (right panel) compared to hadron decays and model calculations (line codes and errors as in Fig. 5).



## 5.2. Invariant transverse momentum spectra of $e^+e^-$ -pairs

The invariant differential pair transverse momentum spectra ( $p_t^{ee}$ ) are shown in Figure 8 for masses  $m_{ee} < 0.2 \text{ GeV}/c^2$  and  $m_{ee} > 0.2 \text{ GeV}/c^2$  respectively. It can be seen that the Dalitz region with  $m_{ee} < 0.2 \text{ GeV}/c^2$  is well reproduced by the hadron decay *cocktail* without significant contributions from pion annihilation. The steep cut-off below  $p_t^{ee} < 0.4 \text{ GeV}/c$  is due to the minimum transverse momentum cut of  $0.2 \text{ GeV}/c$  for the single electron. The pair transverse momentum distribution for pairs with  $m_{ee} > 0.2 \text{ GeV}/c^2$ , however, is strongly enhanced for pairs with  $p_t^{ee} < 0.6 \text{ GeV}/c$  compared to the *cocktail*. Here, all model calculations (also the one using the vacuum  $\rho$  spectral function) describe the pair transverse momentum spectra reasonably well. Therefore, the shape of the spectrum appears to mostly exhibit the basic feature of  $\pi^+\pi^-$  annihilation rather than medium effects, while the latter affect the shape of the invariant mass spectrum.

## 6. DISCUSSION OF RESULTS

We find, both at  $158 \text{ AGeV}/c$  as well as at  $40 \text{ AGeV}/c$ , that the production of  $e^+e^-$ -pairs with  $m_{ee} > 0.2 \text{ GeV}/c^2$  is significantly enhanced as compared to expectations from hadron decays. Moreover, the enhancement is larger at  $40 \text{ AGeV}/c$  compared to  $158 \text{ AGeV}/c$ . In both cases, theories based on  $\pi^+\pi^-$  annihilation are only able to describe the data, if medium modifications of the  $\rho$  propagator are included [ 15, 16, 17, 18].

Comparison of the two energies sheds light on the interesting question whether changes in the properties of the  $\rho$  propagator are more sensitive to changes in the temperature or changes of the baryon density as favored by theory [ 15, 16, 17, 18]. In order to evaluate the  $e^+e^-$ -rates one would need complete knowledge of the dynamical evolution of the fireball. There is no direct handle on the time spent in the various stages of the collision (with the exception of the emission duration of at most 2-3 fm/c and the thermal freeze-out time of 6-8 fm/c from HBT measurements [ 19, 21]). The evolution in terms of temperature and baryochemical potential can, however, be determined at chemical and thermal freeze-out. At chemical freeze-out the total baryon density can be estimated from statistical model calculations fitted to measured particle ratios. It is found to be approximately 0.75 in units of normal nuclear matter density  $\rho_0$  at associated temperatures of 168(145) MeV for 158(40) AGeV/c [ 22]. The baryon density at thermal freeze-out can be derived from the measured HBT-radii [ 19, 20, 21] and rapidity densities [ 23]. It is 0.34(0.53) at temperatures of 120(120) MeV for 158(40) AGeV/c. Note that after chemical freeze-out these baryon densities are all below  $\rho_0$ . Adding in results on initial baryon densities from transport calculations [ 24], the baryon density appears to be consistently higher all the way along the fireball trajectory at the lower beam energy, including a part before reaching chemical equilibrium.

Theoretical calculations which evolve the system through such higher baryon densities are in agreement with the observed increased enhancement at the lower beam energy [ 18]. Taken together, these observations therefore support the importance of coupling the  $\rho$  propagator in the medium to baryon density rather than temperature.

The TPC calibration for the 2000 data has been completed; the analysis of the large number of events taken at the full SPS energy is about to start. With this data it should also be possible to study the behavior of the  $\omega$  and the  $\phi$ . It would further be interesting

to compare the invariant mass spectrum of  $\pi^+\pi^-$ -pairs [ 25] to that from  $e^+e^-$ -pairs, which may allow to discriminate between earlier and later stages of the collision.

## 7. ACKNOWLEDGMENTS

We are grateful for support by the German BMBF, the U.S. DoE, the Israeli Science Foundation, and the MINERVA Foundation.

## REFERENCES

1. F. Karsch, Nucl. Phys. **A698**(2002)199c.
2. J.D. Bjorken, Phys. Rev. **D17**(1983)140.
3. CERN Press Release, CERN 2000-02-07.
4. G. Agakichiev et al. (CERES collaboration), Nucl. Inst. Meth. **A371**(1996)16.
5. A. Marín et al., Nucl. Phys. **A661**(1999)673c.
6. H. Appelshäuser et al. (CERES collaboration), Nucl. Phys. PA698(2002)253c.
7. K. Filimonov et al. (CERES collaboration), Proc. Int. Nucl. Phys. Conf., Berkley 2001, `nucl-ex/0109017`; S. Damjanović, K. Filimonov et al. (CERES collaboration), Proc. CHEP, Budapest 2001, `nucl-ex/0111009`; S. Damjanović et al. (CERES collaboration), 4th ICPAQGP, Jaipur 2001, to appear in Pramana J. Phys..
8. S. Damjanović, Doctoral Thesis, University of Heidelberg (2002); D. Adamová et al., submitted to Phys. Rev. Lett.; `nucl-ex/0209024`.
9. G. Agakichiev et al. (CERES collaboration), Phys. Lett. **B422**(1998)405.
10. G. Agakichiev et al. (CERES collaboration), Nucl. Phys. **A638**(1998)159c.
11. B. Lenkeit et al. (CERES collaboration), Nucl. Phys. **A661**(1999)23c.
12. G. Agakichiev et al. (CERES collaboration), manuscript in preparation.
13. G. Agakichiev et al. (CERES collaboration), Eur. Phys. J. **C4**(1998)231.
14. G. Hering, Doctoral Thesis, University of Darmstadt, 2002; `/nucl-ex/0203004`.
15. G. Brown, M. Rho, Phys. Rep. **363**(2002)85.
16. R. Rapp, J. Wambach, Eur. Phys. J. **A6**(1999)415.
17. R. Rapp, J. Wambach, Adv. Nucl. Phys. **25**(2000)1; R. Rapp, G. Chanfray, J. Wambach, Phys. Rev. Lett. **76**(1996)368, Nucl. Phys. **A617**(1997)472.
18. R. Rapp, Proc. 4th ICPAQGP, Jaipur 2001, to appear in Pramana-J. Phys., `hep-ph/0201101`, and private communication (2001).
19. H. Tilsner, H. Appelshäuser et al. (CERES collaboration), these proceedings.
20. D. Adamová et al. (CERES collaboration), submitted to Phys. Rev. Lett.;`nucl-ex/0207008`.
21. D. Adamová et al. (CERES collaboration), accepted for publication in Nucl. Phys. **A**; `nucl-ex/0207005`.
22. P. Braun-Munzinger, J. Stachel, J. Phys. **G28**(2002)1971.
23. I.G. Bearden et al. (NA44 collaboration), submitted to Phys. Rev. **C**; `nucl-ex/0202019`; M. van Leeuwen et al. (NA49 collaboration), theses proceedings.
24. B. Friman, W. Nörenberg, V.D. Toneev, `nucl-th/9711065`.
25. P. Facchini et al. (STAR collaboration), these proceedings.